

---

---

**STRUCTURE, PHASE TRANSFORMATIONS,  
AND DIFFUSION**

---

---

## **Formation of Phases upon the Mechanosynthesis and Subsequent Annealing of Samples of Cementite Composition Alloyed with Chromium and Nickel**

**A. A. Chulkina\*, A. I. Ul'yanov, V. A. Volkov, A. L. Ul'yanov, A. V. Zagainov, and I. A. Elkin**

*Physicotechnical Institute, Ural Branch, Russian Academy of Science, Izhevsk, 426000 Russia*

*\*e-mail: chulkina@ftiudm.ru*

Received June 21, 2017; in final form, September 5, 2017

**Abstract**—Using X-ray, Mössbauer, and magnetic measurements, the formation of phases has been investigated upon mechanosynthesis in a ball planetary mill and upon the subsequent annealing of samples of the cementite composition  $(\text{Fe}_{0.95-y}\text{Cr}_{0.05}\text{Ni}_y)_{75}\text{C}_{25}$ , where  $y = 0-0.20$ , which contains two alloying elements (chromium and nickel). It has been shown that, in the mechanosynthesis process, cementite alloyed with chromium and a small amount of nickel and an amorphous phase alloyed with chromium and nickel have been formed. Upon heating above  $300^\circ\text{C}$ , the amorphous phase is crystallized into nickel-enriched cementite. In the process of annealing at higher temperatures, the most nickel-rich cementite decomposes with the formation of austenite. As a consequence, after annealing at medium temperatures, the composition of the alloys contains cementite alloyed mainly with chromium and some amount of alloyed austenite, which can be found in ferromagnetic or paramagnetic states depending on the Ni content. Annealing at  $800^\circ\text{C}$  brings about the complete or partial decomposition of cementite contained in the alloys. The intensity of the decomposition has been determined by the nickel content in the samples.

**Keywords:** mechanosynthesis, cementite, alloying with chromium and nickel, annealing, phase and structural changes, X-ray, Mössbauer, thermomagnetic studies

**DOI:** 10.1134/S0031918X18030031

### INTRODUCTION

The trend of modern materials science is directed towards obtaining nanosized structures in massive materials and steels, which makes it theoretically possible to substantially enhance their strength characteristics. An important structural constituent of carbon steels is cementite. In carbon steels, alloying elements are distributed between ferrite and cementite [1], which exert a marked influence on the mechanical properties of steels. Nowadays, however, the effect of alloying elements on the processes of phase formation under the conditions of mechanosynthesis (MS), when the grain size of phases is in the nanosized range, is not adequately studied. The formation in the MS process of cementite alloyed with carbide-stabilizing elements (Mn or Cr) was investigated in [2, 3]. It was shown that in alloys after annealing at  $400-500^\circ\text{C}$ , cementite with not uniform distribution of an alloying element (i.e., both cementite regions depleted of and enriched with Cr or Mn) was observed. High-temperature annealing result in the equalization of the concentration inhomogeneities of alloying elements in cementite. Alloying with Cr and Mn favors the improved stability of cementite to temperature action.

It is of interest to investigate the process of cementite formation under the MS conditions in the presence of two alloying elements, one of which in equilibrium processes is related to carbide-stabilizing elements and another to non-carbide-stabilizing elements, e.g., chromium and nickel. Despite that Ni is not a carbide-stabilizing element, under nonequilibrium conditions, e.g., upon MS, nickel atoms are capable of replacing some amount of iron atoms in the cementite lattice [4]. Therefore, chromium and nickel can exert an appreciable influence on the processes of formation and alloying of phases under the MS conditions and upon subsequent annealing of cementite composites. It is known that alloying with chromium leads to lowering of the Curie point of cementite and alloying with nickel results in elevation of this point [5]. This fact allows one to obtain additional information on the indicated processes using magnetic methods.

### EXPERIMENTAL

Samples of the composition  $(\text{Fe}_{0.95-y}\text{Cr}_{0.05}\text{Ni}_y)_{75}\text{C}_{25}$ , where  $y = 0, 0.05, 0.10, \text{ and } 0.20$ , were obtained by using MS of powders of the OSCh 13-2-grade carbonyl iron of purity 99.98%, nickel and chromium of

purity 99.9%, and graphite of purity 99.99%. The grain size of the initial iron powder did not exceed 5  $\mu\text{m}$ . The MS of the samples was performed in a Pulverizette-7 planetary ball mill in an argon atmosphere for 16 h. The loaded powder mass was 10 g. Vessels and balls of the mill were made from ShKh15 steel. The diameter of the mill balls was 8 mm. The ratio of the mass of balls to the powder mass was 7 : 1. Percentage of the milled iron in the MS process was 4–6%. The powder samples were annealed on a setup measuring the temperature dependence of the magnetic susceptibility  $\chi(T)$ . This made it possible to estimate the phase composition of the samples both before and after annealing, as well as the Curie temperature of ferromagnetic phases, using magnetic measurements. The magnetic susceptibility is given in relative units obtained by dividing the  $\chi_r$  values at the measurement temperature by the value of  $\chi_{20}$  at a temperature of 20°C. The ac magnetic field amplitude of the setup was 1.25 A/cm at a frequency of 120 Hz, and the rate of heating and cooling of the samples was 30 K/min. The holding time upon annealing was 1 h.

The specific saturation magnetization of the samples was measured on a vibration magnetometer in the maximum magnetizing field 13 kA/cm. X-ray studies were performed on a Miniflex 600 diffractometer in the  $\text{Co K}\alpha$  radiation. Mössbauer spectra were taken at the temperature of liquid nitrogen on a YaGRS spectrometer with a  $^{57}\text{Co}$  source of resonance  $\gamma$  radiation in the Rh matrix in the constant acceleration regime. It should be noted that the methods of phase analysis used in this work prevent the detection of carbon in the unbound state, e.g., graphite.

## RESULTS AND DISCUSSION

An analysis of the phase composition of the samples was conducted using X-ray and Mössbauer studies, as well as by using the results of measuring temperature dependences of the relative magnetic susceptibility  $\chi(T)$  and specific saturation magnetization  $\sigma_s$ . Figure 1 presents information on the phase composition of the samples under investigation in the states after MS and subsequent annealing according to the X-ray phase analysis data.

It can be seen that, in the composition of the mechano-synthesized samples, the main available phases are as follows: cementite ( $\text{Fe}, M)_3\text{C}$  (~50–55 vol %), X-ray amorphous  $\text{Am}(\text{Fe}, M, \text{C})$  phase (~34–40 vol %),  $\chi$  carbide ( $\text{Fe}, M)_5\text{C}_2$  (~8–10) vol %, where  $M = \text{Cr}, \text{Ni}$ , and some amount of unreacted or milled  $\alpha$ -Fe (curves 1, 2, 3, and 4, respectively). The samples were subjected to Mössbauer studies. Since alloying with Cr and Ni can lead to a substantial change in the Curie temperature ( $T_C$ ) of cementite, Mössbauer measurements were conducted at the temperature of liquid nitrogen.

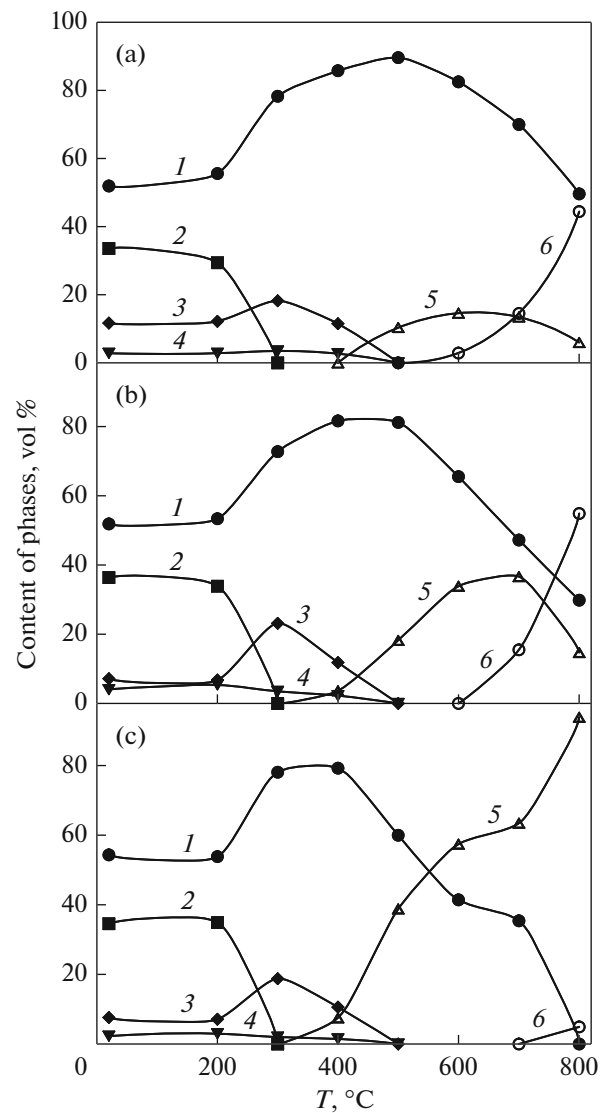


**Fig. 1.** Dependence of the phase composition of composites  $(\text{Fe}_{0.95-y}\text{Cr}_{0.05}\text{Ni}_y)_{75}\text{C}_{25}$ , where (a)  $y = 0.05$ , (b) 0.10, (c) 0.20. Phases: (1) cementite, (2) amorphous phase, (3)  $\chi$  carbide, (4) ferrite, (5) austenite, and (6) martensite.

The results of the Mössbauer studies are shown in Figs. 2 and 3 in the form of a spectrum (left) and a  $P(H)$  function (right), which reflects the distribution of hyperfine magnetic fields at iron atom nuclei. An analysis of the  $P(H)$  function makes it possible to determine phases in the composition of which iron atoms are present. The relative amount of iron atoms in a concrete phase of the sample is calculated from the relative area under the  $P(H)$  function peak of this phase. Figures 2a and 3a display the results of Mössbauer investigations of alloys  $(\text{Fe}_{0.90}\text{Cr}_{0.05}\text{Ni}_{0.05})_{75}\text{C}_{25}$  and  $(\text{Fe}_{0.75}\text{Cr}_{0.05}\text{Ni}_{0.20})_{75}\text{C}_{25}$  in the state after MS. It can be seen that the main fraction of Fe atoms of the samples is accounted for by cementite, for which the

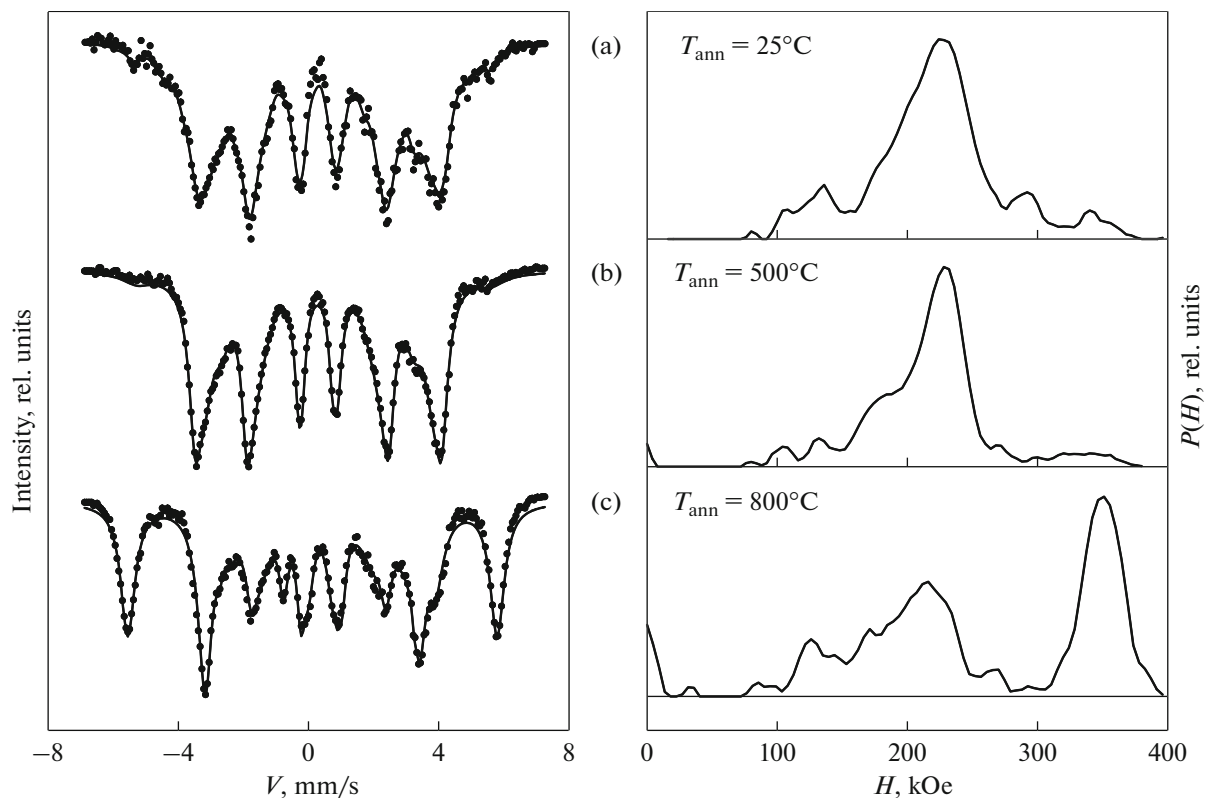


**Fig. 2.** Mössbauer spectra and functions  $P(H)$  of a nanocomposite of the composition  $(\text{Fe}_{0.90}\text{Cr}_{0.05}\text{Ni}_{0.05})_{75}\text{C}_{25}$ : (a) after MS; after annealing at (b) 500 and (c) 800°C.

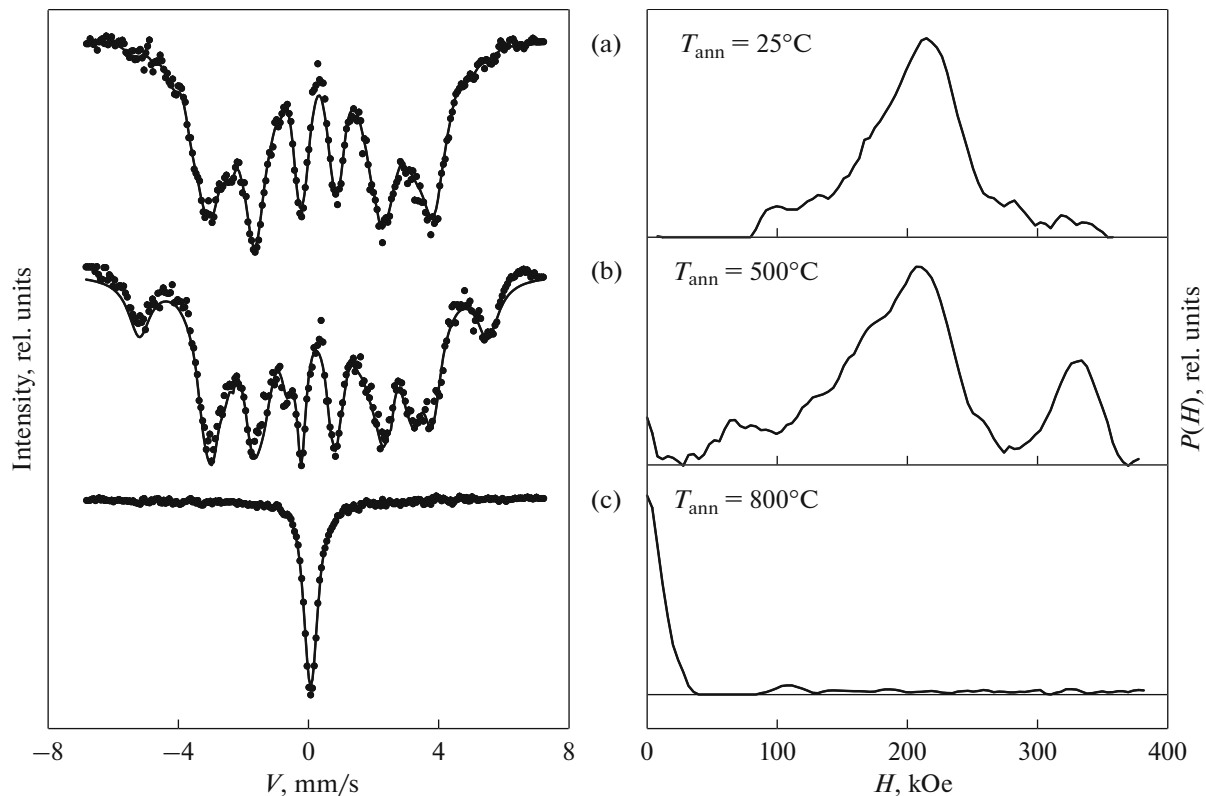


**Fig. 3.** Mössbauer spectra and functions  $P(H)$  of a nanocomposite of the composition  $(\text{Fe}_{0.75}\text{Cr}_{0.05}\text{Ni}_{0.20})_{75}\text{C}_{25}$ : (a) after MS; after annealing at (b) 500 and (c) 800°C.

$P(H)$  function lies in a wide field range  $H = (150\text{--}270)$  kOe and the main maximum falls on the field  $H \approx 220\text{--}230$  kOe. The appearance of asymmetry in the  $P(H)$  function peak of cementite from the side of lower fields indicates the alloying of cementite with chromium [6]. The peaks of the function  $P(H)$  in the field range of 80–150 kOe may be related to carbide  $(\text{Fe}, M)_5\text{C}_2$ . It may also be that the contribution to a broad high-intensity peak of the  $P(H)$  function will come not only from cementite, but also from the amorphous phase, the  $P(H)$  function of which is distributed in the field  $H$  range of 150–320 kOe [7]. The peak in a field  $H \approx 340$  kOe reflects the phase of alloyed  $\alpha$ -Fe. Mössbauer spectra of an alloy  $(\text{Fe}_{0.85}\text{Cr}_{0.05}\text{Ni}_{0.10})_{75}\text{C}_{25}$  are similar to those considered and are not presented in this work. Thus, the Mössbauer measurements qualitatively confirm the results of an X-ray phase analysis of mechanosynthesized alloys.

The phase composition determines the magnitude of specific saturation magnetization  $\sigma_s$  of the indicated samples. It follows from Fig. 4 that, for nanocomposites  $(\text{Fe}_{0.95}\text{Cr}_{0.05})_{75}\text{C}_{25}$  and  $(\text{Fe}_{0.75}\text{Cr}_{0.05}\text{Ni}_{0.20})_{75}\text{C}_{25}$ ,  $\sigma_s$  after MS is 114 and 94 A m<sup>2</sup>/kg (curves 1 and 4, respectively). Based on a comparison of these data with the data on the alloying of cementite with chromium [3], it follows that Ni exerts a weak influence on  $\sigma_s$  of the samples.

The phase composition and degree of alloying of phases of samples after MS and annealing can likewise be judged by the character of dependences of the magnetic susceptibility on the measurement temperature  $\chi(T)$  upon the heating and cooling of samples. Bends or maxima in curves  $\chi(T)$  indicate a transition through the Curie point ( $T_C$ ) of ferromagnetic phases contained in the sample (Fig. 5). Curves 1 in the figure reflect the behavior of temperature dependences of the relative magnetic susceptibility taken upon heating to 800°C; curves 2–5 reflect the behavior upon the cooling of these samples after 1 h of holding at the given annealing temperatures  $T_{\text{ann}} = 300, 400, 500,$  and 800°C. (Curves 1 and 5 in Fig. 5 are shown to a temperature  $T = 600^\circ\text{C}$ ). It can be seen that, on curve 1 in the vicinity of  $T \approx 150^\circ\text{C}$ , the maximum that arises upon a transition from the ferromagnetic state to the paramagnetic state has been observed. The Curie temperature of cementite can be judged by the position of this maximum. It can be seen from Fig. 5 that the fall-off of curve 1 in the region  $150 < T < 300^\circ\text{C}$ , compared to curves 2–4 for the annealed samples, is extended in the measurement temperature. This can be caused by strong distortions of the mechanosynthesized cementite crystal lattice [7], as well as by the transition through the Curie point of the ferromagnetic amorphous phase, the  $T_C$  of which is supposedly close to  $T_C$  of cementite.

In addition, Fig. 5a contains curve 1' measured upon the heating of a mechanosynthesized sample of

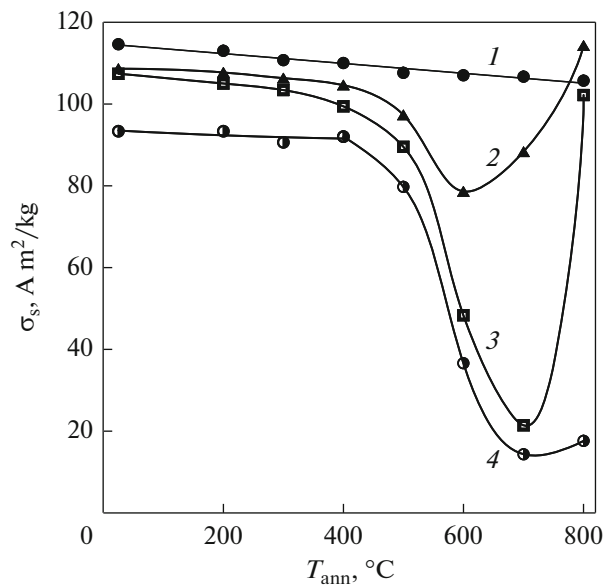
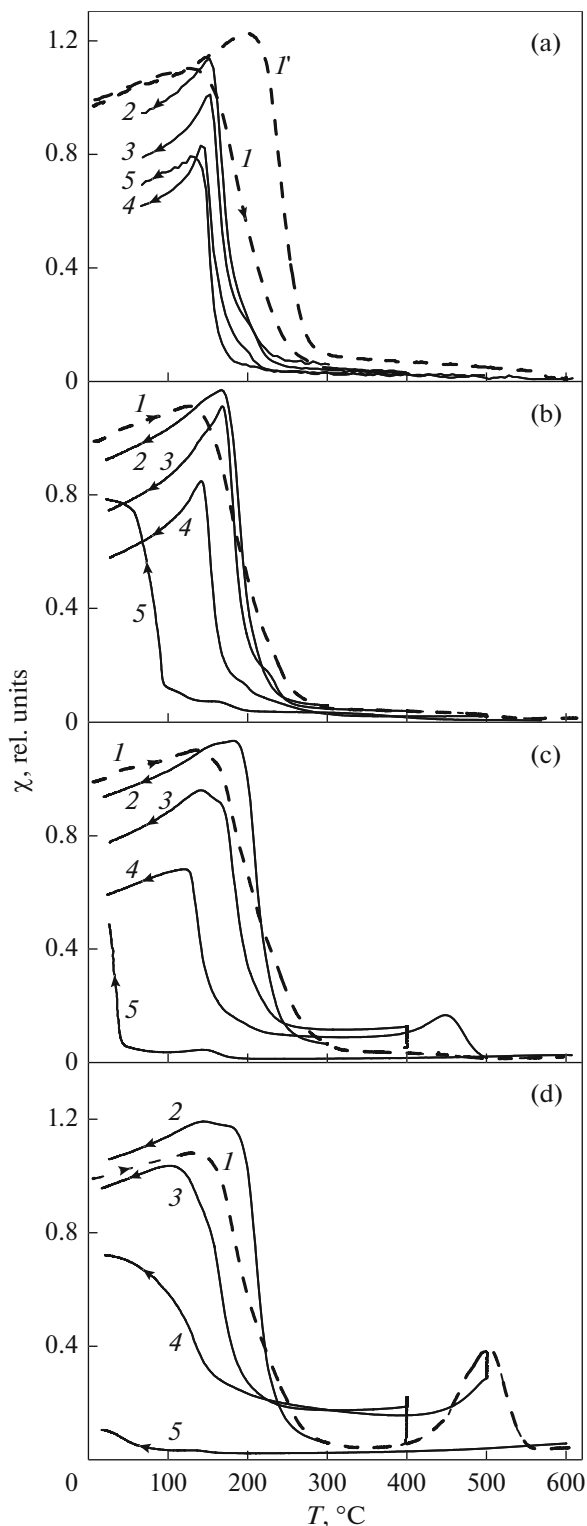


Fig. 4. Dependence of specific saturation magnetization  $\sigma_s$  on annealing temperature of alloys  $(\text{Fe}_{0.95-y}\text{Cr}_{0.05}\text{Ni}_y)_{75}\text{C}_{25}$ , where (1)  $y = 0$ , (2) 0.05, (3) 0.10, and (4) 0.20.

the  $\text{Fe}_{75}\text{C}_{25}$  composition (unalloyed cementite) and curve 1 of a sample of the  $(\text{Fe}_{0.95}\text{Cr}_{0.05})_{75}\text{C}_{25}$  composition, in which 5% Fe atoms are replaced by chromium. It can be seen from a comparison of these curves that the maximum in curve 1 is shifted towards lower temperatures by approximately 50 K. This means that cementite of the  $(\text{Fe}_{0.95}\text{Cr}_{0.05})_{75}\text{C}_{25}$  composition in the state after MS is alloyed with chromium. It follows from Figs. 5b–5d that the maxima in curve 1 of these alloys and the maximum of curve 1 in Fig. 5a fall at the same temperature. This means that cementite with different nickel content after MS is alloyed with chromium alike and, if alloyed with nickel, to an insignificant extent only. It can be assumed that, in the MS process, chromium atoms are uniformly distributed over all phases and nickel atoms are mainly dissolved in the amorphous phase.

In annealing process, at 300°C, the nickel-enriched amorphous phase of mechanosynthesized samples crystallizes with the formation of cementite and some amount of  $\chi$  carbide (Fig. 1, curves 1–3), which are also enriched with Ni. The structural phase changes that occurred in alloys upon the indicated annealing are reflected in curve 2 of dependences  $\chi(T)$  in Fig. 5. The crystallization of the amorphous phase and the partial release of crystal-lattice distortions in the annealing process lead to the fact that transition of cementite from the paramagnetic state to the ferromagnetic state after annealing at 300°C even occurs in a narrower temperature range (cf. Fig. 5, curves 1 and 2). In addition, in curve 2 of the reverse motion of dependences  $\chi(T)$  for samples with  $y \geq 0.05$ , there are two bends, one of which is observed near



**Fig. 5.** Temperature dependences of relative magnetic susceptibility  $\chi$  of mechanosynthesized alloys  $(\text{Fe}_{0.95-y}\text{Cr}_{0.05}\text{Ni}_y)_{75}\text{C}_{25}$ , where (a)  $y = 0$  [3], (b) 0.05, (c) 0.10, (d) 0.20 in the process of heating (curves *I*) and cooling of the same samples but after annealing at temperatures: (curve 2) 300, (3) 400, (4) 500, (5) 800°C. Curve *I'* is a function  $\chi(T)$  in the process of heating an alloy  $\text{Fe}_{75}\text{C}_{25}$  [7].

150°C, while the second is observed in the vicinity of 190°C (Figs. 5c, 5d). On an enlarged scale, these dependences are shown in Fig. 6a. This figure contains a dependence  $\chi(T)$  for a sample of the  $(\text{Fe}_{0.95}\text{Cr}_{0.05})_{75}\text{C}_{25}$  composition, i.e., cementite alloyed with chromium only (curve *I*). Two bends in curves 2–5 in Fig. 6a indicate that the composition of samples after annealing at 300°C contains cementite with different Curie points and, hence, with different contents of alloying elements. The first bend in curve 2 in Figs. 5b–5d falls at a temperature of 150°C. The Curie temperature of cementite alloyed with chromium only exhibits much the same value (Fig. 5a, curve 2). It follows from this that the composition of the alloys annealed at 300°C contains some amount of the cementite formed in the MS process and alloyed mainly with chromium. Mechanosynthesized cementite is supposedly also alloyed with nickel, but to a much lesser extent than in alloying with Cr.

Cementite that arose due to the crystallization of the amorphous phase is alloyed with both chromium and nickel, and alloying with nickel is to a greater extent than in mechanosynthesized cementite. This is evinced by a shift in the second bend in curves  $\chi(T)$  towards higher temperatures [4]. However, alloying this cementite with nickel is likewise limited, as demonstrated by the close values of the Curie temperature of cementite in samples with increasing Ni content (Fig. 6a, curves 3, 4). Indeed, it follows from Fig. 6a that, as the Ni ( $y = 0\text{--}0.10$ ) content in the alloys grows,  $T_C$  of cementite increases from 150 to 190°C (curves *I*–3) and remains unaltered upon further growth of the nickel content (curves 3, 4).

Annealing at 400°C results in the following phase changes (Fig. 1). Part of the carbide  $(\text{Fe,Cr,Ni})_5\text{C}_2$  phase transforms into cementite (curves 3). The start of decomposition of the most nickel-rich regions of cementite leads to the appearance of austenite alloyed with Ni (curves 5). Due to the dominance of the first process over the second one, the total amount of cementite in samples reaches maximum values or approaches them (curves *I*, 3).

The decomposition of the most Ni-rich regions of cementite appeared due to the crystallization of the amorphous phase should lead to the lowering of the Curie point and, hence, to the shift of the bend in the  $\chi(T)$  curves towards lower temperatures. Indeed, after annealing at 300°C, bends in curves 3–4 were near  $T \approx 190^\circ\text{C}$  (Fig. 6a) and, after annealing at 400°C, they were in the range of 160–170°C (Fig. 6b). Decomposition of Ni-enriched cementite leads to a decrease in the susceptibility  $\chi$  in the temperature range of 150–170°C (Fig. 6b, curves 2–4).

It follows from an analysis of the dependences  $\chi(T)$  that, after annealing at 400°C,  $T_C$  of cementite formed in the MS process likewise shifts towards lower temperatures compared to annealing at 300°C. The stronger the shift of bends in the  $\chi(T)$  curves, the larger



amount of nickel is contained in the composition of the alloys (curves 1–4 in Fig. 6b in the temperature range of 110–150°C). This phenomenon can be explained as follows. In the alloys under study, chromium atoms amount to 5% of Fe and Ni atoms. This means that chromium atoms, even on average, are not located in each unit cell (16 atoms) of the cementite lattice. On average, the number of nickel atoms in the cementite lattice can be the same or greater depending on the Ni content in the alloy. In the annealing process at 400°C, volumes of cementite, in unit cells of the lattices of which Cr atoms are absent and the maximum number of Ni atoms are present, primarily decompose. The considered process results in growth of the chromium concentration in cementite, which brings about lowering of its Curie temperature and, hence, a shift of curves  $\chi(T)$  towards lower temperatures.

It can be seen from the dependences  $\sigma_s(T_{\text{ann}})$  presented in Fig. 4 that, in the annealing temperature range up to 400°C, the specific saturation magnetization of the composites changes insignificantly. Apparently, this is connected with the fact that, in the considered annealing temperature range, the main constituents of the composites are cementite, the amorphous phase, and  $\chi$  carbide alloyed with Ni and Cr (Fig. 1), which exhibit close values of  $\sigma_s$ .

Analogous but more significant phase changes occur in the annealing process of alloys at  $T_{\text{ann}} = 500^\circ\text{C}$ . In particular, judging by the X-ray data, alloyed  $\chi$  carbide of samples transforms completely into cementite (Fig. 1, curve 3). In addition, the complete decomposition of cementite that arose upon the crystallization of the amorphous phase, i.e., nickel-enriched cementite, takes place. This is evinced by the disappearance of the second bend in  $\chi(T)$  curves from the side of higher temperatures (Fig. 5, curves 4). As the result of decomposition of Ni-enriched cementite, there forms an austenite whose amount grows with an increase in the nickel content in the alloy composition (Fig. 1, curves 5). Bends in curves 4 continue to shift towards lower measurement temperatures, which indicates the higher degree of alloying of cementite with chromium. This is also favored by the mobility (rather high at  $T_{\text{ann}} = 500^\circ\text{C}$ ) of atoms of alloying elements, which likewise can lead to enrichment of cementite with chromium and austenite with nickel [8]. An analogous phenomenon was observed in [9] upon the tempering of quenched steel 4340 (C = 0.40, Ni = 1.78, and Cr = 0.79 wt %), where the redistribution of Cr atoms from the ferrite matrix into cementite precipitates and Ni atoms from cementite into the ferrite was detected.

The alloying of cementite with chromium after annealing at 500°C is reflected in the Mössbauer spectra. Annealing at 500°C greatly releases the crystal-lattice distortions of cementite, which results in the narrowing of the spectral lines and the  $P(H)$  function peak of cementite. Alloying cementite with chromium

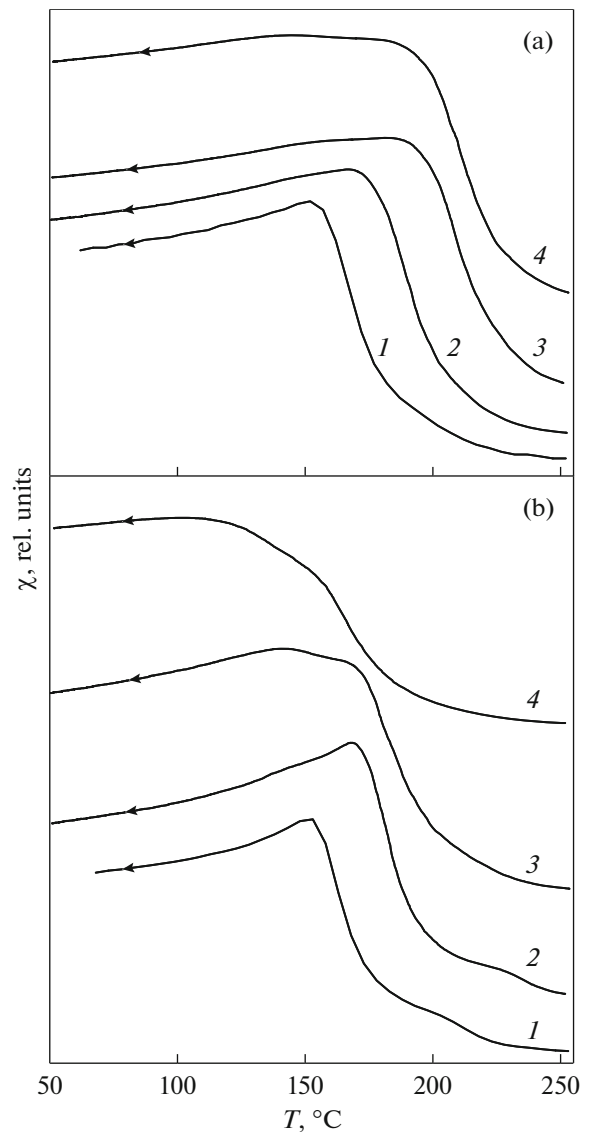


**Fig. 6.** Dependences of relative magnetic susceptibility  $\chi$  on cooling temperature of samples of alloys  $(\text{Fe}_{0.95-y}\text{Cr}_{0.05}\text{Ni}_y)_{75}\text{C}_{25}$ , where (1)  $y = 0$ , (2) 0.05, (3) 0.10, and (4) 0.20 annealed at temperatures (a) 300 and (b) 400°C.

leads to the asymmetric broadening of the  $P(H)$  function peak in the range of fields  $H$  of 130–200 kOe. When alloying cementite with chromium is increased, the number of possible combinations of Ni and Cr atoms in the nearest neighborhood of iron atom grows and each combination yields an additional peak of the function  $P(H)$ , which leads to the appearance of asymmetry of the central peak of the function  $P(H)$  of cementite from the side of low fields. It follows from Figs. 2b and 3b that the asymmetry of the function  $P(H)$  of cementite in an alloy with  $y = 0.20$  compared to a low-nickel alloy ( $y = 0.05$ ), is much stronger. This means the more enhanced alloying of cementite with chromium in the alloy with  $y = 0.20$ .

Noteworthy are the maxima in dependences  $\chi(T)$  in the temperature range of 400–500°C taken upon heating (Fig. 5d, curve 1) an alloy with a high Ni content ( $y = 0.20$ ) or upon cooling an alloy with  $y = 0.10$  after annealing at 500°C (Fig. 5c, curve 4). The appearance of these maxima is connected with the fact that, in high-nickel alloys, the decomposition of most Ni-rich regions of cementite with the formation of austenite takes place even in the heating process, whereas in low-nickel alloys, decomposition occurs after 1-h holding of samples upon annealing. Depending on the nickel content, austenite can be ferromagnetic (Ni > 30 at %) or paramagnetic (Ni < 30 at %) [10]. As follows from Figs. 5c and 5d, at least some of the austenite is in the ferromagnetic state, as evinced by the nonzero value of the magnetic susceptibility  $\chi$  in curves 3 and 4 in the temperature range of 500–400 to 200°C. The position of maxima in curves 4 (Fig. 5c) and 1 (Fig. 5d) in the temperature range of 450–500°C actually reflects the Curie temperature of austenite, based on which the Ni content in it can be judged. Estimates of samples with  $y = 0.10$  and 0.20 made according to [11] yield an Ni content in austenite of 42 and ~50 at %, respectively. It should be noted that, in [11], an Fe–Ni alloy was considered. The presence of extra Cr and C in the composition of the samples under study can somewhat shift the Curie point of austenite. The appearance of austenite in the samples after annealing at 500°C is likewise fixed in the X-ray (curve 5 in Fig. 1) and Mössbauer (Figs. 2b, 3b) data. A feature of Mössbauer studies is the possibility of reliable determination of paramagnetic austenite. It follows from an analysis of the  $P(H)$  function of the Mössbauer spectra of the alloys annealed at 500°C (Figs. 2b, 3b) that, in their composition, along with cementite (the  $P(H)$  function peak in the field of  $H = 220$  kOe), a small amount of paramagnetic austenite is also contained (the  $P(H)$  function peak in a field of  $H = 0$  kOe). In ferromagnetic austenite, functions  $P(H)$  are distributed in a wide magnetic-field range (20–300) kOe [10] and, hence, overlap the function  $P(H)$  of cementite. In explicit form, a part of the function  $P(H)$  of ferromagnetic austenite is revealed in a sample with a high nickel content ( $y = 0.20$ ) in the range of fields  $H$  from 20–100 kOe (Fig. 3b). When analyzing the Mössbauer data, it is necessary to take into account the fact that samples in the process of measurement were in the temperature of liquid nitrogen at which austenite  $\gamma$  (Fe,Cr,Ni,C) additionally undergoes martensitic transformation. Indeed, according to the X-ray data, after annealing at 500°C the composition of the sample with high nickel content ( $y = 0.20$ ) includes two phases, i.e., cementite and austenite (Fig. 1, curves 1, 5). At the same time, in this sample, according to the Mössbauer data, the pronounced  $P(H)$  function peak in the field  $H \approx 340$  kOe is observed, which can be identified as low-carbon martensite or  $\alpha$  Fe alloyed with Ni (Fig. 3b). This means that, in the process of Mössbauer measure-

ments at the temperature of liquid nitrogen, a good part of austenite of the sample underwent the martensitic transformation. In a sample with low nickel content ( $y = 0.05$ ) the  $P(H)$  function peak of martensite manifests weakly (Fig. 2b). Thus, the Mössbauer measurements qualitatively confirm the X-ray data on the phase composition of the samples after annealing at 500°C.

The appearance of nonferromagnetic austenite in the composition of samples annealed at 500°C and the decomposition of part of the cementite in samples with high nickel content bring about some decrease in the specific saturation magnetization of all these samples (Fig. 4).

Annealing at higher temperatures bring about the further decomposition of cementite (Fig. 1, curves 1), including cementite alloyed with chromium. In this case, the stability of cementite under the action of temperature decreases, as the nickel content in the composition of samples increases. For example, after 1-h annealing at 800°C, the cementite content in samples of the composition  $(\text{Fe}_{0.95-y}\text{Cr}_{0.05}\text{Ni}_y)_{75}\text{C}_{25}$ , where  $y = 0.05, 0.10,$  and  $0.20$  is 50, 30, and 0 vol %, respectively. As was shown above, after MS, the content of nickel dissolved in cementite is limited. It is possible that, after MS, some part of Ni atoms proportional to the nickel content in samples is in the bulk of cementite grains in the form of clusters, finely dispersed nickel inclusions, or some other constituents. Upon high-temperature annealing, these Ni atoms acquire mobility sufficient for their dissolution in the cementite lattice, which simultaneously alloys cementite and stimulates its decomposition. This process can take place as demonstrated by the elevation of  $T_C$  of cementite in alloys annealed at 800°C compared to annealing at 500°C. This can be observed in the dependences  $\chi(T)$  of an alloy  $(\text{Fe}_{0.85}\text{Cr}_{0.05}\text{Ni}_{0.10})_{75}\text{C}_{25}$  presented in Fig. 5c. It can be seen that the Curie temperature of cementite of the alloy annealed at 500°C is ~120°C (curve 4) and  $T_C \approx 150^\circ\text{C}$  after annealing at 800°C (curve 5). The low value of the magnetic susceptibility of cementite in curve 5 is due to the fact that, after high-temperature annealing, cementite becomes low magnetic, as will be discussed below. The analogous picture (possibly less pronounced) is observed for the alloy  $(\text{Fe}_{0.90}\text{Cr}_{0.05}\text{Ni}_{0.05})_{75}\text{C}_{25}$  (Fig. 5b).

As the annealing temperature increases, the amount of austenite in the samples grows. At the same time, with an increase in the nickel content, in the composition of samples the fraction of austenite underwent decreases in the martensitic transformation (Fig. 1, curves 5). This can be explained because alloying with nickel stabilizes austenite and shifts the martensitic transformation towards a range of lower temperatures.

Mössbauer measurements on samples annealed at 800°C with allowance for the fact that these were conducted at the temperature of liquid nitrogen qualita-

tively confirm the X-ray data. It follows from an analysis of the  $P(H)$  function of an alloy with  $y = 0.05$  (Fig. 2c) that the composition of the sample contains cementite (the main peak of the function  $P(H)$  in a field of 220 kOe), which is highly alloyed with chromium (asymmetry of the peak from the side of lower fields). Along with cementite, the composition of the sample contains martensite (the  $P(H)$  function peak in a field 350 kOe) and some amount of paramagnetic austenite (the  $P(H)$  function peak in a field  $H = 0$  kOe). After annealing at 800°C of a sample with high Ni content ( $y = 0.20$ ), we observe practically one phase: paramagnetic austenite (the  $P(H)$  function peak in a field  $H = 0$  kOe in Fig. 3c).

The phase changes that occurred at  $T_{\text{ann}} = 800^\circ\text{C}$  are reflected in the dependences  $\chi(T)$  of alloys (Fig. 5, curves 5). After annealing an alloy with  $y = 0.05$ , martensite alloyed with Ni with a Curie temperature  $\sim 60^\circ\text{C}$  becomes a ferromagnetic phase with the greatest saturation magnetization (Fig. 5b, curve 5). In an alloy with a higher Ni content ( $y = 0.10$ ), the  $T_C$  of martensite approaches room temperature (Fig. 5c, curve 5). The decomposition of cementite in an alloy with a high Ni content ( $y = 0.20$ ) leads to the appearance in the composition of the sample of almost one phase, i.e., paramagnetic austenite, which reflects in the dependence  $\chi(T)$  as the near-zero value of the magnetic susceptibility (Fig. 5d, curve 5).

The above results are supported by the measurements of dependences  $\sigma_s(T_{\text{ann}})$  of alloys (Fig. 4). Cementite alloyed only with chromium is stable in the entire range of annealing temperatures, and its specific saturation magnetization varies slightly (Fig. 4, curve 1). Alloying mechanosynthesized samples of the cementite composition with chromium and nickel leads to substantial changes in the phase composition of composites in the annealing temperature range of 500–800°C, which is reflected in the dependences  $\sigma_s(T_{\text{ann}})$ . We will consider this in greater detail.

In curve 2 (Fig. 4) of an alloy with an Ni content of  $y = 0.05$ , the minimum is observed in the neighborhood of  $T_{\text{ann}} = 600^\circ\text{C}$ . According to the data of Fig. 1a, the composition of the alloy annealed at this temperature contains 82 vol % cementite, about 4 vol % austenite, and 4 vol % ferromagnetic martensite, the saturation magnetization of which is the highest of all the considered phases. The minimum in the  $\sigma_s(T_{\text{ann}})$  curve at  $T_{\text{ann}} = 600^\circ\text{C}$  is due to the fact that austenite alloyed with Ni and formed upon decomposition of cementite is largely in the paramagnetic state. After annealing at 800°C, the alloy composition contains only 45 vol % of the ferromagnetic martensite (Fig. 1, curve 6) with the result that  $\sigma_s$  of the sample increases anew (Fig. 4, curve 2). In an alloy with  $y = 0.10$ , the minimum in the dependence  $\sigma_s(T_{\text{ann}})$  falls on a temperature of 700°C (Fig. 4, curve 3). According to the data of Fig. 1b, at this temperature, the alloy contains 48 vol % cementite, 14 vol % ferromagnetic marten-

site, and 38 vol % paramagnetic austenite. Despite the large volume of ferromagnetic phases (cementite and martensite), the specific saturation magnetization of the sample is comparatively small ( $\sim 24 \text{ A m}^2/\text{kg}$ ). The analogous phenomenon after annealing at 700°C is also observed in the alloy with  $y = 0.20$  (Fig. 4, curve 4), in which 36 vol % of cementite is contained and the rest is mainly paramagnetic austenite (Fig. 1c, curves 1, 5). In our opinion, this phenomenon is caused by the low  $\sigma_s$  value of cementite which is the result of additional alloying of cementite with nickel in the process of high-temperature annealing.

After annealing of a sample with  $y = 0.10$  at 800°C, the content of paramagnetic austenite and low-magnetic cementite decreases to 14 and 31 vol %, respectively, whereas the ferromagnetic martensite content increases sharply to 55 vol % (Fig. 1b, curves 5, 6), which leads to intense growth in  $\sigma_s$  for the alloy (Fig. 4, curve 3).

In an alloy with high Ni content ( $y = 0.20$ ), annealing at 700–800°C lead to the decomposition of a major portion of cementite with the formation of mostly nonferromagnetic (Fig. 3c) austenite (Fig. 1c, curves 1, 5). The low  $\sigma_s$  value in curve 4 in the range of  $T_{\text{ann}} = 700\text{--}800^\circ\text{C}$  (Fig. 4) is due to the presence of small amounts of ferromagnetic phases in samples, i.e., martensite and, possibly, ferromagnetic (Fig. 5d, curve 5) austenite (Fig. 1c, curves 1, 6).

## CONCLUSIONS

(1) It has been shown that, due to MS of powders of the composition  $(\text{Fe}_{0.95-y}\text{Cr}_{0.05}\text{Ni}_y)_{75}\text{C}_{25}$ , where  $0 \leq y \leq 0.20$ , samples contain the following phases: cementite, amorphous phase, and some amount of  $\chi$  carbide. Cementite after MS is mainly alloyed with chromium. Nickel likewise dissolves in cementite, but in a limited amount. The amorphous phase is alloyed with nickel to a greater degree than with chromium.

(2) It has been found that cementite and  $\chi$  carbide, which arises in the process of the crystallization of the amorphous phase upon low-temperature annealing (300°C), are alloyed with nickel to a larger degree than after MS. As a consequence, after the low-temperature annealing, the alloy composition contains two types of cementite one of which appeared in the MS process and is mainly alloyed with chromium. The other type of cementite is formed from the amorphous phase in the annealing process and, compared to mechanosynthesized cementite, is enriched with nickel. The two types of cementite differ in the Curie temperature.

(3) It has been shown that annealings in the temperature range of 400–500°C give rise to the decomposition processes of the most nickel-rich cementite. As this takes place, the undecomposed cementite is enriched with chromium.



(4) Annealing at higher temperatures bring about the further decomposition of cementite, including cementite alloyed with chromium. In high-nickel alloys, due to the decomposition of cementite, austenite alloyed with Cr and Ni is actively formed. Depending on the nickel content, austenite can be in ferromagnetic or paramagnetic states. In the annealing temperature range of 500–600°C, the redistribution of alloying elements takes place; in particular, chromium (carbide-forming element) passes from austenite to cementite. In alloys with  $\gamma < 0.20$ , upon high-temperature (700–800°C) annealing, the dissolution of nickel in the cementite lattice grows.

#### ACKNOWLEDGMENTS

This work was performed under a State Assignment of the Federal Agency of Scientific Organizations of Russia (project no. AAAA-A16-116021010085-9) and was supported in part by the Ural Branch of the Russian Academy of Sciences (project no. 15-6-2-16).

#### REFERENCES

1. G. Miyamoto, J. C. Oh, K. Hono, T. Furuhashi, and T. Maki, "Effect of Partitioning of Mn and Si on the Growth Kinetics of Cementite in Tempered Fe–0.6 mass % C Martensite," *Acta Mater.* **55**, 5027–5038 (2007).
2. A. I. Ul'yanov, A. A. Chulkina, and V. A. Volkov, E. P. Elsukov, A. V. Zagainov, A. V. Protasov, and I. A. Zykina, "Structural State and Magnetic Properties of Cementite Alloyed with Manganese," *Fiz. Met. Metallogr.* **113**, 1134–1145 (2012).
3. A. A. Chulkina, A. I. Ul'yanov, V. A. Zagainov, A. L. Ul'yanov, and E. P. Elsukov, "Formation of Chromium-Alloyed Cementite in the Process of Mechano-synthesis and Subsequent Annealings," *Fiz. Met. Metallogr.* **116**, 293–301 (2015).
4. A. I. Ul'yanov, A. A. Chulkina, V. A. Volkov, A. L. Ul'yanov, and A. V. Zagainov, "Structure and Magnetic Properties of Mechanically Synthesized  $(\text{Fe}_{1-x}\text{Ni}_x)_{75}\text{C}_{25}$  Nanocomposites," *Fiz. Met. Metallogr.* **118**, 691–699 (2017).
5. T. Shigematsu, "Magnetic Properties of Cementite  $(\text{Fe}_{1-x}\text{Me}_x)_3\text{C}$ , (Me; Cr or Ni)," *J. Phys. Soc. Jpn.* **37**, 940–946 (1974).
6. A. L. Ul'yanov, A. I. Ul'yanov, A. A. Chulkina, and E. P. Elsukov, "Mössbauer Studies of the Formation of Cr-Doped Cementite during Mechanochemical Synthesis and Subsequent Annealings," *Bull. Rus. Acad. Sci.: Phys.*, No. 8, 1026–1030 (2015).
7. E. P. Elsukov, G. A. Dorofeev, V. M. Fomin, G. N. Konygin, A. V. Zagainov, and A. N. Maratkanova, "Mechanically Alloyed  $\text{Fe}(100-x)\text{C}(x)$  ( $x = 5-25$  at %) Powders: I. Structure, Phase Composition, and Temperature Stability," *Fiz. Met. Metallogr.* **94**, 356–366 (2002).
8. M. A. Smirnov, V. M. Schastlivtsev, and L. G. Zhuravlev, *Osnovy termicheskoi obrabotki stali* (Izd-vo UrO RAN, Ekaterinburg, 1999) [in Russian].
9. C. Zhu, X. Y. Xiong, A. Cerezo, R. Hardwicke, G. Krauss, and G. D. W. Smith, "Three-Dimensional Atom Probe Characterization of Alloy Element Partitioning in Cementite During Tempering of Alloy Steel," *Ultramicroscopy* **107**, 808–812 (2007).
10. V. A. Shabashov, V. V. Sagaradze, A. V. Litvinov, and A. E. Zamatovskii, "Relaxation of the Structure of Fe–Ni Alloys during Mechanical Alloying Induced by Severe Plastic Deformation," *Fiz. Met. Metallogr.* **116**, 869–878 (2015).
11. E. E. Yurchikov, A. Z. Menshikov, and V. A. Tzurin, "Mössbauer Study of the Magnetic Transformation in  $\gamma$ -FeNi Alloys," in *Proc. Conf. on the Application of the Mössbauer Effect*, Tihany, 1969, pp. 405–411.

*Translated by I. Krasnov*